
EFDA–JET–CP(04)03-53

J.D. Strachan, J.P. Coad, G. Corrigan, G.F. Matthews, and J. Spence
and JET EFDA Contributors

EDGE2D Simulations of JET ¹³C Migration Experiments

EDGE2D Simulations of JET ^{13}C Migration Experiments

J.D. Strachan¹, J.P. Coad², G. Corrigan², G.F. Matthews², and J. Spence²
and JET EFDA Contributors and JET EFDA Contributors*

¹PPPL, Princeton University, PO Box 451, Princeton NJ 08543, USA

²EURATOM/UKAEA Fusion Association, Culham Science Centre, Abingdon, Oxon, OX14 3DB, UK

* See annex of J. Pamela et al, "Overview of Recent JET Results and Future Perspectives",
Fusion Energy 2002 (Proc. 19th IAEA Fusion Energy Conference, Lyon (2002).

Preprint of Paper to be submitted for publication in Proceedings of the
31st EPS Conference,
(London, UK. 28th June - 2nd July 2004)

“This document is intended for publication in the open literature. It is made available on the understanding that it may not be further circulated and extracts or references may not be published prior to publication of the original when applicable, or without the consent of the Publications Officer, EFDA, Culham Science Centre, Abingdon, Oxon, OX14 3DB, UK.”

“Enquiries about Copyright and reproduction should be addressed to the Publications Officer, EFDA, Culham Science Centre, Abingdon, Oxon, OX14 3DB, UK.”

INTRODUCTION.

Material migration has received renewed interest due to tritium retention associated with carbon transport to remote vessel locations [1]. Those results influence the desirability of carbon usage on ITER. Subsequently, additional experiments have been performed, including tracer experiments attempting to identify material migration from specific locations. In this paper, EDGE2D models a well-diagnosed JET ^{13}C tracer migration experiment [2]. The role of SOL flows upon the migration patterns is identified.

The JET ^{13}C migration experiments [2] were performed as the final experiment of the 2001 campaign. This experiment has several modelling advantages since a single plasma condition, equilibrium, and machine configuration was used, and the SOL was well diagnosed. The lack of ELMs in the ohmic heated plasma also facilitates the modelling. The ^{13}C was introduced into the vessel at the main chamber top at a single toroidal location, and the ^{13}C was observed measured in the divertor plates along the field lines connected to the location of the methane injection (Fig.1). The toroidal localization of the ^{13}C injection and detection hinders quantitative comparison with the modelling.

The results (Fig.1) indicated the carbon was deposited entirely on the inner divertor target, displaced from the strike point in the SOL direction (Fig.2). That pattern also generally occurs for campaign-integrated deposition of main chamber material [e.g.3]. By contrast, campaign-averaged migration of divertor material consists of erosion from the outer strike point and deposition at the inner strike point [e.g.4]. Sometimes, divertor material has been found dispersed throughout both inner and outer target surfaces [5].

Separately, JET observed SOL flows directed towards the inner divertor [6]. Consequently, the inner target material accumulation has been attributed to the SOL flows [1]. That attribution was re-enforced by JET reversed field experiments where the SOL flow was changed and co-deposited layers grew near the outer strike point [7].

This paper reports modelling of the carbon migration pattern for carbon injected at the same location as the ^{13}C JET experiment and for carbon injected at the outer strike point location. EDGE2D [8] solves the fluid equations along a grid derived from the experimental plasma equilibrium. Carbon impurities are introduced as atoms and are followed during their neutral state by the Monte Carlo code NIMBUS. The atomic species can be introduced as specified puffed sources or as sputtered sources with rates dependent upon the chemical and physical sputtering coefficients used. Here, sputtered carbon was not allowed and only the carbon from the machine top or outer strike point was introduced. In this manner, the migration pattern of the injected carbon was evident.

To isolate the influence of the SOL flows, we follow the treatment used to describe the experimental carbon screening [9] in the JET normal and reverse field experiments [10]. SOL flows similar to the experimental values were induced using an external force whose origin is not specified. Since the physical origin of the JET SOL flows is presently not known, they cannot be included in EDGE2D by first-principles calculations. We used the external force to create the flows and then use the EDGE2D calculations to understand the influence of the flows upon the carbon

migration. The force was applied to the low field side of the plasma extending up to the vessel top, and to a 2cm depth just outside the separatrix. The force could be applied either to the deuterium ions alone, or to both the deuterium and carbon ions. The magnitude of the force was adjusted until the flow at the machine top approximated the JET measurements. In the case of the force acting upon the deuterium ions only, the carbon flow is altered significantly by the collisional drag with the deuterons. The calculations with the force acting also upon the carbon assumed a force per carbon equal to the force per deuteron. The distribution of the force over the charge states was assumed in proportion to the charge state density. Due to the higher density of deuterium than carbon, the total force on the deuterium was about ten times the total force on the carbon.

When carbon was injected at the machine top, then the carbon migration pattern indicated the preferred destination was the inner target, but that the relative magnitude related to the SOL flow direction (Fig.2 and 3). A factor of twelve more carbon migrated to the inner divertor when the SOL flow was directed towards the inner divertor. When the flow was near stagnation (reverse field case), then twice as much carbon migrated to the inner compared to the outer divertor leg. Some carbon was observed to flow to the outer divertor leg, even when the SOL flow was towards the inner divertor leg. This latter observation conflicts with the ^{13}C experiment where less than 1% of the carbon was deposited on the outer targets [2]. The deposition pattern along the target was distributed on the SOL side away from the strike point (Fig.2) much as was observed both in the JET ^{13}C and campaign-averaged migration of main chamber material. Both the experimental and EDGE2D results are expressed in terms of the flux to the vertical, since the EDGE2D grid edge does not exactly reproduce the actual divertor plates. The minimum of the experimental carbon fluence at about 24cm from the strike point is located near a ridge in the divertor plate. Plausibly re-erosion might most effect that data location, and re-erosion effects are not included in EDGE2D. The high deposition at 29cm above the strike point is on the divertor baffle.

When the carbon was injected at the outer strike point, then greater than 90% of the carbon was re-deposited near the outer strike point (Fig.4). EDGE2D is not particularly suited for the prompt re-deposition calculation, so the pattern and quantity of the re-deposition is qualitative. The carbon, which does migrate, escapes to the main chamber SOL due to the thermal force pulling the carbon out of the divertor region. That carbon was re-deposited away from the strike point (Fig.4 and 5), in a manner similar to the top injected carbon. As for the top injection, the carbon deposited away from the strike point was about twelve times more likely to migrate to the inner divertor for flows directed towards the inner divertor, and about twice as likely to migrate to the inner divertor for flows which stagnated at the vessel top. Less total carbon was migrated from the outer strike point when the flow was directed towards the inner target. Apparently, that flow allowed divertor plasma conditions which led to less carbon escape than with the stagnated (reverse field flow). No deposition was found in the vicinity of the inner strike point in contrast to the campaign averaged experimental results for divertor material migration. The deposition with the flow towards the inner target did result in a deposition closer to the inner strike point (Fig.4).

Unlike for the carbon screening [9], the migration distribution to the inner/outer divertors was influenced by the SOL flows but the deposition pattern inside the inner divertor was unchanged because the carbon escape into the divertor was dominated by the friction and thermal forces and not changed by the SOL flow. Possibly re-erosion [11] influenced by target temperature, which was not calculated in EDGE2D, must be viewed as a candidates to explain the deposition pattern on the inner target and the small deposition on the outer target.

REFERENCES

- [1]. J.P.Coad, et al, J. Nucl. Mater. **290-293**, 224 (2001)
- [2]. J. Likonen, et al, Fus. Eng. And Design **66-68**, 219 (2003)
- [3]. W.R.Wampler, et al, J. Nucl. Mater. **266-269**, 217 (1999)
- [4]. Y. Gotoh, et al, J. Nucl. Mater. **313-316**, 370 (2003)
- [5]. K. Krieger, et al, J. Nucl. Mater. **313-316**, 327 (2003)
- [6]. S.K.Erents, et al, Plasma Phys Control. Fusion **42**, 905 (2000)
- [7]. P.Andrews, et al, 16th PSI Conference (Portland, Maine, 2004)
- [8]. R. Simonini, et al, Contrib. Plasma Phys. **34**, 368 (1994)
- [9]. J.D.Strachan, et al, 16th PSI Conference (Portland, Maine, 2004)
- [10]. R.A. Pitts, et al, 16th PSI Conference (Portland, Maine, 2004)
- [11]. K. Ohya, Jap. J. Appl. Phys. **42**, 5769 (2003)

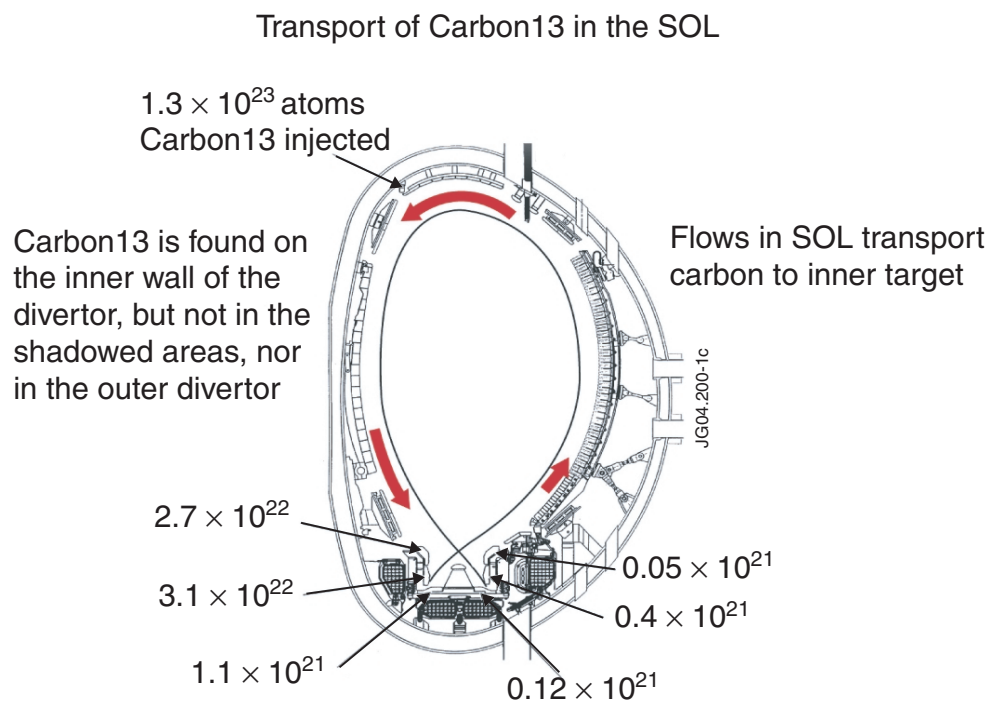


Figure 1: Schematic diagram with JET ¹³C results, and indicating with arrows the direction of the JET SOL flow

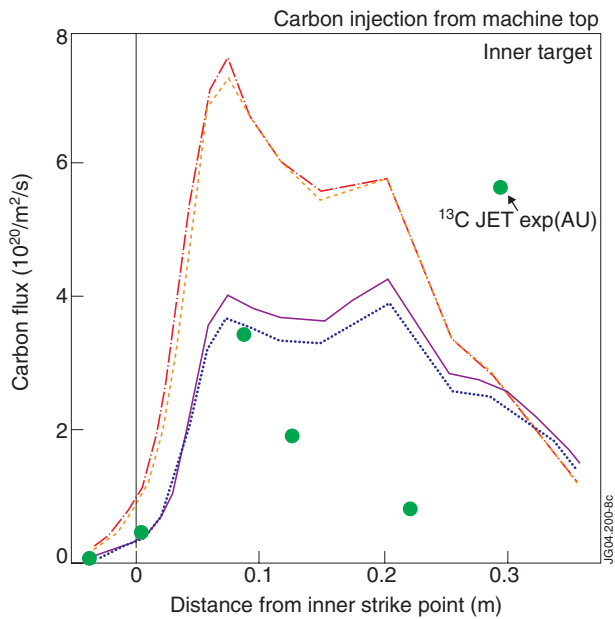


Figure 2: EDGE2D deposition on inner target with carbon injected from vessel top. The four cases include the force acting on the D alone or D and carbon (orange or purple), for forward (red) and reverse flows(blue).

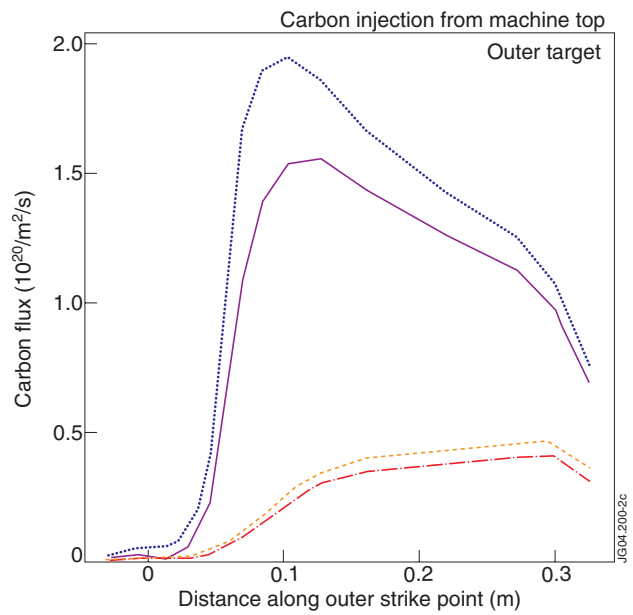


Figure 3:EDGE2D deposition on outer target with carbon injected from vessel top. Colors are the same as in Figure 2.

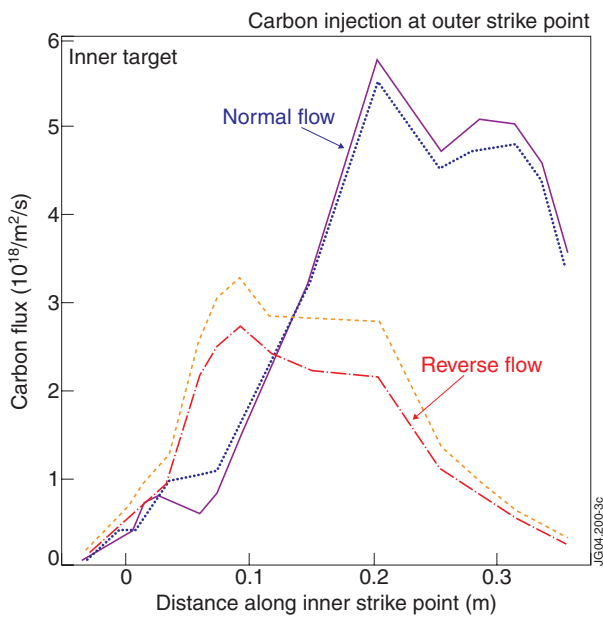


Figure 4: Carbon deposition on inner target with carbon injected at outer strike point.

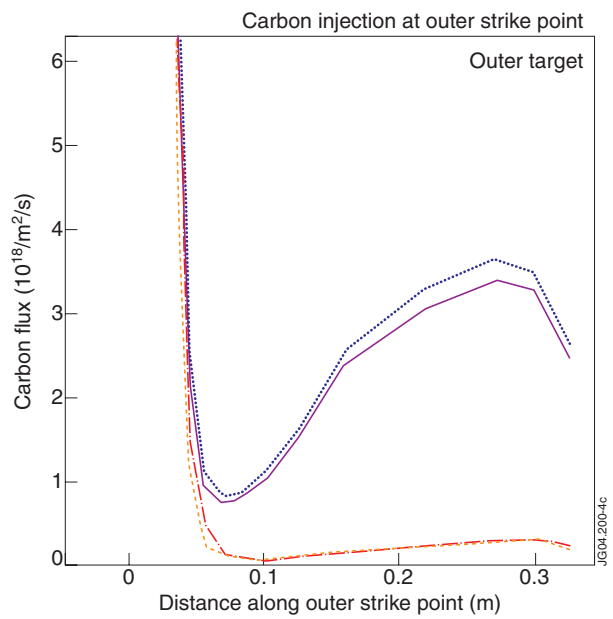


Figure 5: Carbon deposition on outer target with carbon injected at outer strike point.